ACS OMEGA

http://pubs.acs.org/journal/acsodf

Article

Improving the Yield of Xenocoumacin 1 Enabled by In Situ Product Removal

Yijie Dong, Xiaohui Li, Jiaqi Duan, Youcai Qin, Xiufen Yang, Jie Ren, and Guangyue Li*

Cite This: *ACS Omega* 2020, 5, 20391−20398

Read Online

ACCESS | Metrics & More | Article Recommendations | Supporting Information

ABSTRACT: Xenocoumacin 1 (Xcn1), a major antimicrobial compound produced by *Xenorhabdus nematophila* CB6, has great potential to be developed into a novel biofungicide. However, its low yield in the producing cells has limited its possible commercial applications. In this study, we explored the effect of in situ product removal (ISPR), a well-established recovery technique, with the use of macroporous resin X-5 on the production of Xcn1 in a fermentation setting. Relative to the routine fermentation process, the yield of Xcn1 was improved from 42.5 to 73.8 μg/mL (1.7-fold) and 12.9 to 60.3 μg/mL (4.7-fold) in three and ten days, respectively. By agar diffusion plate and growth inhibition assays, the antibiotic activity against *Bacillus subtilis* and *Alternaria solani* was also found to be improved. Further study revealed that protection of Xcn1 against degradation and decrease in cell self-toxicity as well as upregulation of biosynthesis-related genes of Xcn1 at the transcription level contributed to yield improvement of Xcn1. In addition, resin X-5 significantly altered the metabolite profile of *X. nematophila* CB6, which could promote the discovery of new antibiotics.

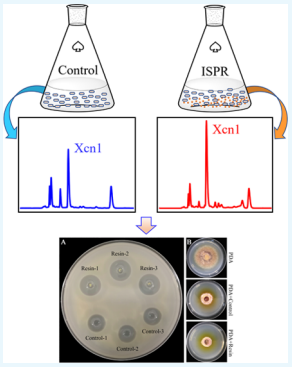

INTRODUCTION

Xenorhabdus nematophila, a type of motile Gram-negative bacteria, lives in symbiosis with the entomopathogenic nematode *Steinernema carpocapsae*.[1−3] These bacteria colonize in a specialized intestinal receptacle of the infective juvenile (IJ) form of the nematode, and together, they form an entomopathogenic complex that can infect and kill different insects.[2,4−6] To survive, the nematodes search for a susceptible insect host in soil, perforating the insect's intestinal wall and migrating into the hemocoel. Once in the hemocoel, the nematode releases *X. nematophila* into the insect host's hemolymph, and the bacteria produce immunosuppressive compounds and insect toxins to overcome the host immune system and kill it.[7−11] As colonies of *X. nematophila* proliferate to a high cell density, they secrete exoenzymes that degrade insect tissues and antibiotics for suppressing the growth of microbial competitors.[12−20] *S. carpocapsae* then propagates in the hemocoel feeding on *X. nematophila* as well as the nutrients derived from the insect source. With the depletion of nutrients, the nematodes develop into the IJ stage; thereafter, they emerge from the insect cadaver into the soil in search for a new insect host.[3,4,21]

In the life cycle of the entomopathogenic *S. carpocapsae*−*X. nematophila* complex, *X. nematophila* produces several compounds with antimicrobial activity, including indole derivatives, nematophin, benzylideneacetone, xenocoumacins, and nonribosomal produced secondary metabolites.[1,17,19,22−29] Among them, the water-soluble peptide antimicrobial compounds, Xcns, such as xenocoumacin 1 (Xcn1, $C_{22}H_{35}N_5O_6$) and xenocoumacin 2 (Xcn 2, $C_{21}H_{30}N_2O_6$) shown in Figure 1, are the major antibiotics produced in the broth culture by *X. nematophila*.[30,31] Biosynthesis of Xcns is associated with a 39 kb cluster of 14 genes that include two nonribosomal peptide synthetases (NRPS) and three polyketide synthases (PKSs) (Figure S1).[32] Although both Xcns show antimicrobial activity, Xcn1 is much more active in its antifungal activity. However, the accumulation of Xcn1 is toxic to the producing cells. To avoid self-toxicity *X. nematophila* had evolved a resistance mechanism by converting Xcn1 to the weaker antibiotic Xcn2.

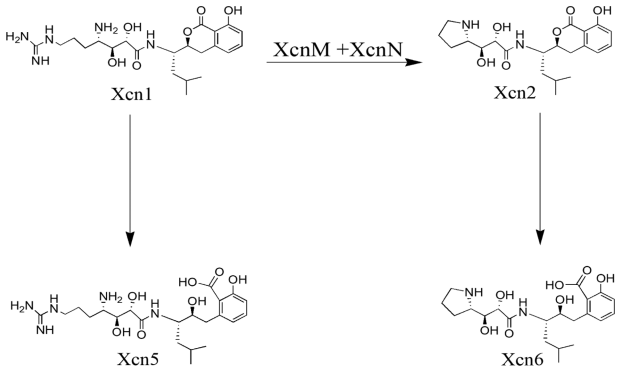

Figure 1. Proposed conversion pathways among Xcn1, Xcn2, Xcn5, and Xcn6 as reported previously.[35]

Received: May 20, 2020
Accepted: July 20, 2020
Published: August 3, 2020

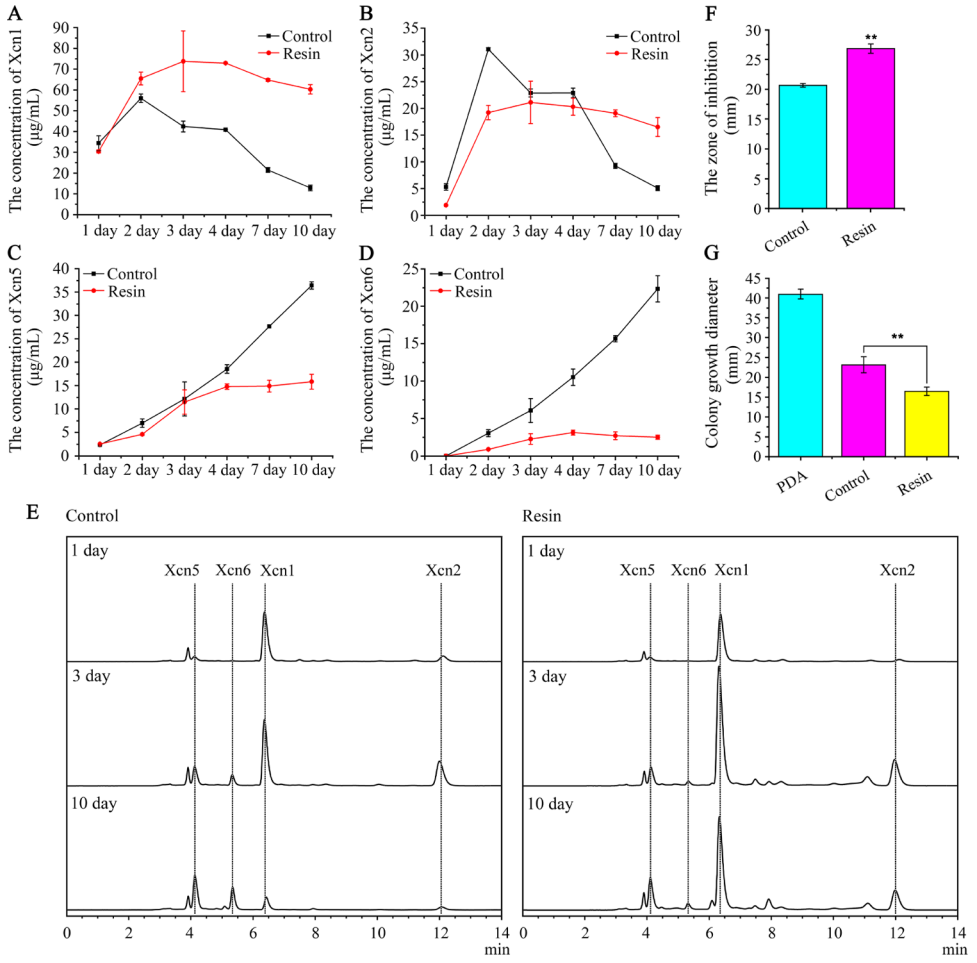

Figure 2. Effects of adsorber X-5 on yields of Xcn1 and its derivatives. (A) Concentration dynamic curve of Xcn1 detected by high-performance liquid chromatography (HPLC) during the fermentation process. (B) Concentration dynamic curve of Xcn2. (C) Concentration dynamic curve of Xcn5. (D) Concentration dynamic curve of Xcn6. (E) HPLC analysis of Xcn1 and its derivatives in the fermentation process, and all chromatograms are normalized based on the same ratio. (F) Antibacterial activity of isolated compounds from the culture of *X. nematophila* CB6 against *B. subtilis*. The clear zone surrounding the well was measured for comparing the inhibiting effect. Control, the compounds were extracted from the culture of *X. nematophila* CB6 by adding 2% (v/v) of resin X-5 to the harvested supernatant after fermentation; resin, the compounds were extracted from the culture of *X. nematophila* CB6 by adding 2% (v/v) of resin X-5 to the CLB medium before fermentation. (G) Antifungal activity of isolated compounds from the culture of *X. nematophila* CB6 against *A. solani* measured by the growth inhibition assay. The colony growth diameter of *A. solani* on the potato dextrose agar (PDA) plate was measured for comparing the inhibiting activity. PDA, *A. solani* grown on the PDA plate; control, *A. solani* grown on the PDA plate containing the compounds extracted as described above; resin, *A. solani* grown on the PDA plate containing the compounds extracted as described above.

The responsible genes are *xcnM* and *xcnN*, which encode proteins homologous to saccharopine dehydrogenases and fatty acid desaturases, respectively.[32−34] On the other hand, Xcn1 and Xcn2 can be hydrolyzed to Xcn5 and Xcn6, respectively (Figure 1), which is another detoxification pathway.[35]

Prompted by the broad-spectrum antibiotic activity of Xcn1, Yang et al. explored its potential as a novel fungicide for biocontrol of *Phytophthora infestans*[36] that causes potato late blight disease. Potato late blight disease is one of the most devastating plant diseases worldwide, which destroyed potato crops in Europe in the 1840s and caused mass starvation.[37] Currently, *P. infestans* is still one of the major pathogens targeted by chemical companies searching for new fungicides. Yang et al. showed that Xcn1 not only inhibited mycelial growth of *P. infestans*, reaching 100% inhibition at 1.5 μg/mL Xcn1, but also suppressed sporangia production. Additionally, Xcn1 also exhibits strong antifungal activity against other species of *Phytophthora*, with EC_{50} values ranging from 0.25 to 4.17 μg/mL.[36,38] To sum up, Xcn1 possesses great potential to be developed into a novel biofungicide utilized for plant protection. However, the detoxification mechanism leading to the degradation of Xcn1 prevents its accumulation in the fermentation process, therefore limiting its commercial applications.

In situ product removal (ISPR) involves the immediate separation of a product from its producing cells; therefore, it could improve the yield of the product via two possible effects: minimization of interference resulting from product accumulation from the producing cells and minimization of product losses caused by the cross interaction with the enzymes produced by the producing cells and environmental conditions.[39,40] In addition, this technique could also simplify the downstream processing steps.[41] To date, most studies involving ISPR focused on acetone, butanol, and ethanol as well as organic acid fermentation with organic solvents, ion-exchange resins, and adsorbent polymers as the widely used separation materials.[42,43]

https://dx.doi.org/10.1021/acsomega.0c02357
ACS Omega 2020, 5, 20391−20398

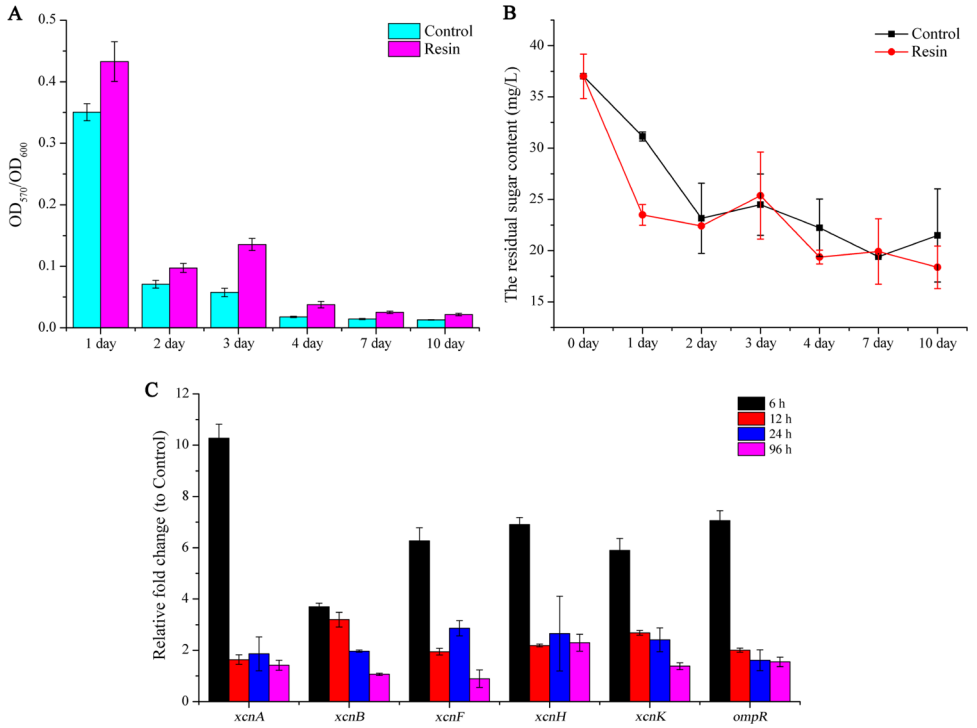

Figure 3. Effect of X-5 on the cellular metabolic process and Xcn1-biosynthesis-related gene transcription of *X. nematophila* CB6. (A) Metabolic activity of *X. nematophila* CB6 in treatment and control measured by the 3-(4,5-dimethylthiazol-2-yl)−2,5-diphenyltetrazolium bromide (MTT) assay. (B) Reducing sugar concentration during fermentation was measured by the 3,5-dinitrosalicylic acid (DNS) method. (C) Relative transcription level of Xcn1-biosynthesis-related genes (*xcnA*, *xcnB*, *xcnF*, *xcnH*, *xcnK*, and *ompR*) was measured by real-time quantitative polymerase chain reaction (RT-qPCR), and all of the data were normalized based on the expression of *recA*. Data was shown as means ± standard errors (SEs).

In this study, ISPR based on macroporous resins was explored in the fermentation process of *X. nematophila* CB6 to improve the yield of Xcn1. In addition, the underlying reasons for an improved yield were also explored.

RESULTS AND DISCUSSION

Improving the Yield of Xcn1 by In Situ Product Removal. Helped by Xcn1, which exhibits a broad-spectrum antibiotic activity against bacteria and several fungal species, *X. nematophila* could efficiently protect the nutrient resources of the insect cadaver against food competitors from soil microorganisms, while excess Xcn1 is also toxic against the producer itself. As a result, accumulated Xcn1 during fermentation could activate a defense mechanism of *X. nematophila* to avoid self-toxicity by converting Xcn1 to weak antibiotic Xcn2 and other related derivatives, which would limit the commercial process of Xcn1 production.[35] In addition, to the best of our knowledge, there is no chemical route reported for the synthesis of Xcn1 or its derivatives. Therefore, in an attempt to improve the yield of Xcn1, ISPR, an efficient method for rescuing the fermentation process limited by inhibitory or toxic products as well as unstable products, was employed to limit the conversion from Xcn1 to Xcn2 as well as other derivatives. In routine cultivation, the yield of Xcn1 as well as Xcn2 reached a plateau in two days, then decayed rapidly, and dropped to quite a low level in ten days (Figures 2A,B,E and S2A). Xcn5 and Xcn6 appeared after the formation of Xcn1 and Xcn2 and then continued to accumulate in significant amounts following the consumption of Xcn1 and Xcn2 in ten days (Figures 2C−E and S2A), which is in line with the proposed conversion pathways in Figure 1. However, in cultures grown with resin X-5, the yield of Xcn1 increased significantly in the first three days and then kept at a relatively high level in the following seven days (Figures 2A and S2B). The yield of Xcn1 treated with X-5 was increased from 42.5 to 73.8 μg/mL (1.7-fold) and 12.9 to 60.3 μg/mL (4.7-fold) with respect to the control on the third and tenth day, respectively. Correspondingly, low levels of Xcn5 and Xcn6 were observed in the treatment (Figures 2C−E and S2B), suggesting that resin X-5 somehow protected Xcn1 and Xcn2 against conversion or degradation. Next, we carried out the agar diffusion plate assay and the growth inhibition assay against *Bacillus subtilis* and *Alternaria solani*, respectively, to test whether the higher yield of Xcn1 gave a corresponding greater antibiotic activity. As expected, in comparison with the control, the zone of inhibition against *B. subtilis* increased from 20.7 to 26.8 mm (Figures 2F and S3A), while the colony growth diameter of *A. solani* decreased by 6.8 mm in resin X-5 treatment (Figures 2G and S3B), indicating higher antibiotic activity.

Effect of ISPR on Metabolic Activity and Gene Expression of *X. nematophila* CB6. Prompted by the improved yield of Xcn1 in ISPR treatment, we tested the effect of X-5 on cell density and metabolic activity, both of which could contribute to the yield of Xcn1. Our experimental data from a fermentation process revealed that X-5 affected the growth of *X. nematophila* CB6, resulting in a decreased cell density (Figure S4). It is postulated that the adsorption of X-5 for medium components and intermediate metabolites of *X. nematophila* CB6 during fermentation interfered with the growth of *X. nematophila* CB6. Therefore, it might be cell metabolic activity rather than cell density that improved the

https://dx.doi.org/10.1021/acsomega.0c02357
ACS Omega 2020, 5, 20391−20398

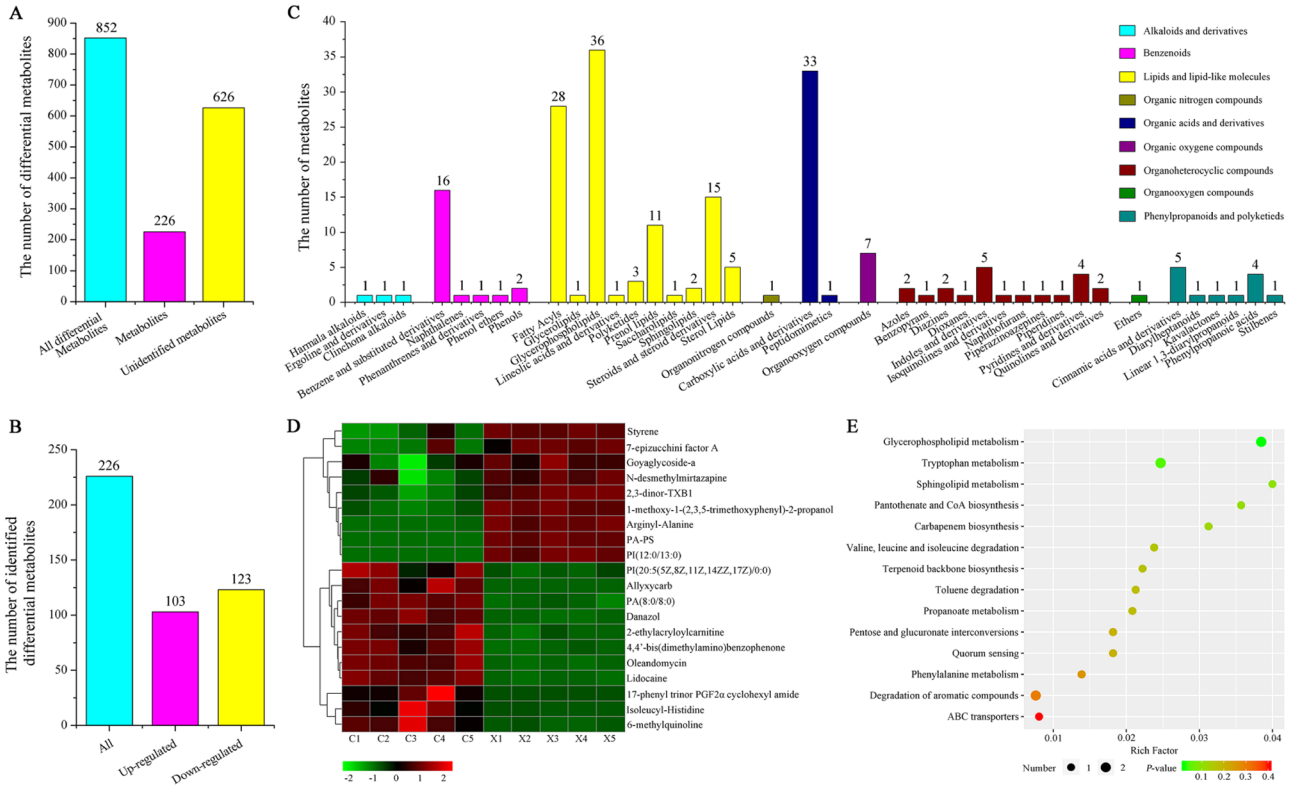

Figure 4. Untargeted metabolomic analysis of the metabolite profile of *X. nematophila* CB6 treated by resin X-5. (A) Classification of total differential metabolites. (B) Classification of 226 identified differential metabolites. (C) Distribution of differential metabolites based on chemical classification. (D) Hierarchically clustered heatmap of differential metabolites. (E) Scatter plot of differential metabolites enriched in the KEGG pathway.

yield of Xcn1. The former appeared to be the case since the metabolic activity of *X. nematophila* CB6, grown in the presence of resin X-5, increased remarkably compared to the control (Figure 3A). However, in both control and treated samples, the respective cell metabolic activity decreased sharply after the second day (Figure 3A). This corresponded to the consumption of reducing sugar (Figure 3B). The yield of Xcn1 reaching a plateau in three days (Figure 2A) appeared to be closely related to the cell metabolic activity of *X. nematophila* CB6 and consumption of reducing sugar. To extend the cell viability, we tried adding glucose on the second day of fermentation. However, no appreciable improvement in the yield of Xcn1 was observed, and the reason is not known at this time.

In the biosynthetic gene cluster of Xcn1, *xcnA* and *xcnK* encoded two nonribosomal peptide synthetases (NRPS); *xcnF*, *xcnH*, and *xcnL* encoded three polyketide synthases (PKSs); and *xcnB*, *xcnC*, and *xcnE* were predicted to be involved in hydroxymalonyl CoA synthesis. We further investigated the effect of resin X-5 on the transcription of some crucial genes in the biosynthetic gene clusters of Xcn1 (Figure S1),[19,32] namely, *xcnA*, *xcnB*, *xcnF*, *xcnH*, and *xcnK*. Relative to the control, transcription of these genes in resin X-5 treatment was upregulated by 3.7−10.3 fold (Figure 3C), consistent with the higher yield of Xcn1. However, transcription of these genes declined evidently after 6 h in the culture process, especially *xcnA*, the NRPS encoding gene of Xcn1 biosynthetic pathway, implying that the biosynthesis of Xcn1 was repressed at the transcriptional level. As a global regulator, OmpR repressed the transcription of *xcnA-L* but enhanced the transcription of *xcnMN* in *X. nematophila*.[32,44] However, the transcription of the *ompR* gene showed a similar trend to *xcnA-L* in the present research, speculating that resin addition might lead to intracellular transcriptional reprogramming. In summary, these results demonstrated that the removal of Xcns by resin remarkably increased cell metabolic activity and also upregulated the transcription of biosynthesis-related genes of Xcn1.

Metabolite Analysis of *X. nematophila* CB6 Treated by Resin X-5. Two unknown products, with retention times being 7.93 and 10.96 min, respectively, were detected by high-performance liquid chromatography (HPLC) due to their remarkably enhanced yield in the resin X-5-treated sample (Figure S5). It was presumed that the positive regulation of operons of specific gene clusters or the limiting effect against metabolite degradation caused by resin X-5 contribute to the accumulation of the two unknown products. Therefore, resin X-5-mediated ISPR might interfere with the metabolic process of *X. nematophila* CB6 and facilitate the discovery of potentially new metabolites. To confirm the phenomenon observed experimentally, an untargeted metabolomic analysis of the extracts was performed by ultrahigh-performance liquid chromatography−mass spectrometry (UPLC−MS). A total of 2943 metabolites were identified in all samples, including 852 differential metabolites based on the criteria of variable influence on projection (VIP) > 1.0 and *P*-value < 0.05 (Table S2 and Figure S6) and 626 differential metabolites appeared to be new (Figure 4A). We analyzed 226 of the known differential metabolites and found that 103 were upregulated and 123 were downregulated (Figure 4B). According to chemical classification, the annotated metabolites could be categorized into nine groups: alkaloids and

https://dx.doi.org/10.1021/acsomega.0c02357
ACS Omega 2020, 5, 20391−20398

derivatives, benzenoids, lipids and lipidlike molecules, organic nitrogen compounds, organic acids and derivatives, organic oxygen compounds, organoheterocyclic compounds, organooxygen compounds, and phenylpropanoids and polyketides (Figure 4C). Interestingly, some dipeptides and nonribosomal peptides, such as arginyl−alanine, mauritine A, sakacin A, enalapril, neuromedin N, and triiodothyronine sulfate, the potential precursor of the antibacterial material, were upregulated by 1.4−32.4 fold due to resin treatment. Sakacin A, which is a class IIa, pediocin-like antilisterial bacteriocin, can inhibit the growth of several lactic acid bacteria and *Listeria monocytogenes*.[45,46] Furthermore, based on the hierarchical clustering analysis, some compounds that possess potential pharmacological activity were significantly upregulated because of resin X-5 treatment (Figure 4D). These include 7-epizucchini factor A, goyaglycoside-a,[47] *N*-desmethylmirtazapine,[48] 2,3-dinor-TXB1,[49] and 1-methoxy-1-(2,4,5-trimethoxyphenyl)-2-propanol. The identified differential metabolites were annotated in the Kyoto Encyclopedia of Genes and Genomes (KEGG) database and enriched in 14 prominent pathways (Figure 4E) that are involved in the biosynthesis and metabolism of amino acids, glycerophospholipids, carbapenem biosynthesis, and quorum sensing. In summary, ISPR treatment remarkably altered the metabolite profile of *X. nematophila* CB6 that resulted in the enrichment of some intermediate metabolites.

CONCLUSIONS

In conclusion, with the help of ISPR, the yield of Xcn1 was improved significantly during the fermentation process, accompanied by an improved antibiotic activity against *B. subtilis* and *A. solani*. The improved yield of Xcn1 apparently resulted from three factors: improvement of the cell metabolic activity of *X. nematophila* CB6 by minimizing Xcn1 accumulation, the protective role of resin X-5 for Xcn1 against conversion or degradation, and upregulation of biosynthesis-related genes of Xcn1 at the transcriptional level. In addition, resin X-5 significantly altered the metabolite profile of *X. nematophila* CB6, especially some dipeptides and nonribosomal peptides. Therefore, the increased antimicrobial activity might be the synergistic effects of these compounds acting together with Xcn1 and its derivatives as well as some still unknown compounds. Finally, we anticipate that the application of ISPR coupled with metabolite engineering could further improve the yield of Xcn1, accelerating the development process of Xcn1 as a new biofungicide in plant protection.

MATERIALS AND METHODS

Strain, Media, and Growth Conditions. *X. nematophila* var. *pekingensis* CB6 was isolated from entomopathogenic nematode *Steinernema* sp. screened from a soil sample in Beijing, China. *B. subtilis* utilized in this study was a strain stored in our lab. *A. solani* was kindly provided by Professor Qinying Wang (Agriculture University of HeBei, China). *X. nematophila* CB6 was inoculated in 5 mL of CLB medium (1.0% tryptone, 0.5% yeast extract, 0.5% NaCl, 0.01 mM $MgSO_4$) and cultured at 30 °C with shaking at 200 rpm for 12 h. The preculture was scaled up to 100 mL of CLB medium at an initial OD_{600} of 0.1 and then incubated for the desired period depending on the type of experiments as follows. *B. subtilis* were grown at 37 °C in liquid LB medium, and *A. solani* were grown at 25 °C on potato dextrose agar (PDA).

Extraction of Xenocoumacin and Its Derivatives. The nonpolar macroporous resin X-5 could efficiently extract Xcn1 and its derivatives from fermentation broth.[50] We employed two conditions for extracting the desired chemicals from the culture of *X. nematophila* CB6: first, 2% (v/v) of resin X-5 was added to 100 mL of CLB medium before fermentation, that is, before inoculating *X. nematophila* CB6; second, resin X-5 was added to the harvested supernatant after fermentation as a control. Resin X-5 was separated from cells and the supernatant by filtration and then extracted twice with MeOH (1 × 100 mL, 1 × 50 mL), and the combined extract was concentrated to dryness using a rotary evaporator. The residue was redissolved in ddH_2O and then filtered through a 0.22 μm pore size syringe microfilter for HPLC analysis. The condition for HPLC analysis is as follows: an Agilent C18 column (4.6 mm × 150 mm), with ddH_2O containing 0.1% formic acid/acetonitrile (70:30) serving as the mobile phase.

Cell Density Assay. For measuring the cell density, the optical density at 600 nm [OD_{600}] of *X. nematophila* CB6 was monitored at predetermined time points. The experiments were done in triplicate.

3-(4,5-Dimethylthiazol-2-yl)-2,5-diphenyltetrazolium Bromide (MTT) Assay. The metabolic activity of *X. nematophila* CB6 was measured by the MTT assay as reported previously.[51] The harvested cells were washed three times with sterilized phosphate-buffered saline (PBS) buffer and then resuspended in the same buffer, following the kit instructions (Beyotime, C0009).

Quantification of Reducing Sugars. The reducing sugar content was determined using the 3,5-dinitrosalicylic acid (DNS) method.[52] The supernatant (1 mL) of culture, collected during fermentation, was mixed with 1 mL of DNS reagent and then heated at 100 °C for 15 min. The absorbance was monitored at 540 nm by an ultraviolet−visible (UV−vis) spectrometer. The content of reducing sugars was determined by comparing it to a standard curve created by glucose at different concentrations.

Real-Time Quantitative PCR (RT-qPCR). The bacterial total ribonucleic acid (RNA) was extracted using the Bacterial RNA Extraction Kit (Vazyme, R403-01). All of the quantitative PCR reactions were performed using SYBR Green qPCR SuperMix (TransGen Biotech, AQ132-14) according to the instructions. PCR conditions are as follows: 95 °C for 30 s, (95 °C for 5 s, 60 °C for 34 s) × 40 cycles. To compare the difference of transcription between the control and resin X-5 treatment, the relative transcription abundance ($\Delta\Delta C_T$) was measured by the formula $\Delta\Delta C_T = \Delta C_T$ (X-5 treatment) − ΔC_T (control), where the relative transcription abundance of the tested gene (ΔC_T) was calculated by $\Delta C_T = C_T$(tested gene) − C_T(reference gene). Relative gene transcription was determined by the $2^{-\Delta\Delta C_T}$ method, and one-way analysis of variance (ANOVA) was performed for analyzing the difference at the statistical level. The RT-qPCR primers for measuring Xcn1 biosynthetic related genes are listed in Table S1.

Antibiotic Activity Assay. The antibacterial activity of the compounds, extracted from the culture of *X. nematophila* CB6, against *B. subtilis* was measured by the agar diffusion plate assay.[53] Sample wells were prepared on a two-layer agar diffusion plate, in which 20 mL of medium containing 0.75% agar and 10^7−10^8 colonies of *B. subtilis* were layered above 10 mL of 2% sterilized agar. The extract (100 μL) prepared as

https://dx.doi.org/10.1021/acsomega.0c02357
ACS Omega 2020, 5, 20391−20398

described above was added to the well, and after 24 h incubation at 37 °C, the clear inhibition zone surrounding the well was measured and compared.

To test the antifungal activity of isolated compounds from *X. nematophila* CB6, an *A. solani* strain that is sensitive to Xcn1 was chosen as a model fungus based on its growth inhibition. Briefly, the tested sample was mixed with the PDA medium with a final concentration of 5 or 10% and then poured onto a Petri dish. The mycelia PDA block was cut from the edges of a three-day colony of *A. solani* growing on PDA and then placed at the center of the plate for culturing at 28 °C. After three days, the diameter of growth inhibition was measured.

Metabolomic Analysis by LC−MS. The metabolomic profiling of the isolated compounds of resin X-5 from *X. nematophila* CB6 under different conditions was analyzed by LC−MS. Specifically, 20 μL of 2-chloro-L-phenylalanine (0.3 mg/mL) dissolved in methanol as an internal standard was added to 1 mL of sample, then lyophilized, and redissolved in 300 μL of methanol/acetonitrile (2:1, v/v). The sample was vortexed for 30 s and placed at 4 °C for 2 min, after which it was centrifuged at 13 000 rpm and 4 °C for 15 min. The supernatant was transferred into a new glass vial and then lyophilized again. The residue was redissolved in 300 μL of methanol and water (1:4, v/v) and filtered through 0.22 μm microfilters for LC−MS analysis. LC−MS was performed on an ACQUITY UPLC system (Waters Corporation, Milford) coupled with an AB SCIEX Triple TOF 5600 System (AB SCIEX, Framingham, MA). The conditions for HPLC separation are as follows: An ACQUITY BEH C18 column (100 mm × 2.1 mm i.d., 1.7 μm; Waters Corporation) is employed in both positive and negative modes; the injection volume is 10 μL; mobile phase A is water containing 0.1% formic acid; mobile phase B is acetonitrile/methanol (2:3, v/v) containing 0.1% formic acid; and the linear gradient is 0 min, 1% B; 1 min, 30% B; 2.5 min, 60% B; 6.5 min, 90% B; 8.5 min, 100% B; 10.7 min, 100% B; 10.8 min, 1% B; and 13 min, 1% B. During separation, the flow rate was 0.4 mL/min and the column temperature was 45 °C. Quality control (QC) samples, which were prepared by pooling aliquots of all of the samples into one, were injected at regular intervals (every ten samples) throughout the analytical run to provide a set of data from which repeatability can be measured.

Metabolite Identification and Statistical Analysis. The acquired LC−MS raw data were converted by Progenesis QI software (Waters Corporation, Milford), as previously described.[54] In this study, we set the parameters as follows: precursor tolerance, 5 ppm; fragment tolerance, 10 ppm; and retention time (RT) tolerance, 0.02 min. Internal standard detection parameters were deselected for peak RT alignment, isotopic peaks were excluded from analysis, the noise elimination level was set at 10.00, and the minimum intensity was set to 15% of the base peak intensity. Finally, the data matrix (.xls) was obtained with three-dimensional data sets including m/z, peak RT, and peak intensity. Each ion was identified by RT−m/z pairs, and the peaks with missing values (ion intensity = 0) in more than 50% of samples were removed from the data matrix. The internal standard was used for QC data. Also, the metabolites were identified by QI Data Processing Software through public databases (http://www.hmdb.ca/, http://www.lipidmaps.org/) and self-built databases.

Principle component analysis (PCA) and orthogonal partial least-squares discriminant analysis (OPLS-DA) were performed for visualizing the differential metabolites between the control and treatment, after mean centering (Ctr) and Pareto variance (Par) scaling, respectively.[55] The default seven-round cross validation was performed to guard against overfitting. The differential metabolites were determined on the basis of the combination of a statistically significant threshold of variable influence on projection (VIP) values obtained from the OPLS-DA model and Student's *t*-test (*P* values) on the normalized peak areas, where metabolites with VIP values larger than 1.0 and *P*-values less than 0.05 were considered as differential metabolites. The pathway annotation analysis was conducted by the compound identification number (CID) in the Kyoto Encyclopedia of Genes and Genomes (KEGG, https://www.genome.jp/kegg/pathway.html) database. Metabolite classification, prominent metabolic pathway detection, and enrichment analyses were also carried out.

■ ASSOCIATED CONTENT

Supporting Information

The Supporting Information is available free of charge at https://pubs.acs.org/doi/10.1021/acsomega.0c02357.

Characterization of Xenocoumacin 1 biosynthesis gene cluster in *X. nematophila* CB6 (Figure S1); ratios of Xcn1 and its derivatives in different cultivation processes (Figure S2); role of resin addition in antibiotic activity (Figure S3); effect of resin addition on growth of *X. nematophila* CB6 (Figure S4); effect of resin X-5 on the yield of two unknown products (Figure S5); quality control of untargeted metabolomic data (Figure S6); list of RT-qPCR primers used in this study (Table S1) (PDF)

Detailed information about all of the metabolites detected in the control and resin group samples (Table S2) (XLSX)

■ AUTHOR INFORMATION

Corresponding Author

Guangyue Li − *State Key Laboratory for Biology of Plant Diseases and Insect Pests/Key Laboratory of Control of Biological Hazard Factors (Plant Origin) for Agri-product Quality and Safety, Ministry of Agriculture, Institute of Plant Protection, Chinese Academy of Agricultural Sciences, Beijing 100081, People's Republic of China;* orcid.org/0000-0002-6320-9624; Email: liguangyue1983@163.com

Authors

Yijie Dong − *State Key Laboratory for Biology of Plant Diseases and Insect Pests/Key Laboratory of Control of Biological Hazard Factors (Plant Origin) for Agri-product Quality and Safety, Ministry of Agriculture, Institute of Plant Protection, Chinese Academy of Agricultural Sciences, Beijing 100081, People's Republic of China; Guangdong Provincial Key Laboratory of Microbial Culture Collection and Application, State Key Laboratory of Applied Microbiology Southern China, Guangdong Institute of Microbiology, Guangdong Academy of Sciences, Guangzhou 510070, People's Republic of China*

Xiaohui Li − *State Key Laboratory for Biology of Plant Diseases and Insect Pests/Key Laboratory of Control of Biological Hazard Factors (Plant Origin) for Agri-product Quality and Safety, Ministry of Agriculture, Institute of Plant Protection,*

https://dx.doi.org/10.1021/acsomega.0c02357
ACS Omega 2020, 5, 20391−20398

Chinese Academy of Agricultural Sciences, Beijing 100081, People's Republic of China

Jiaqi Duan − *State Key Laboratory for Biology of Plant Diseases and Insect Pests/Key Laboratory of Control of Biological Hazard Factors (Plant Origin) for Agri-product Quality and Safety, Ministry of Agriculture, Institute of Plant Protection, Chinese Academy of Agricultural Sciences, Beijing 100081, People's Republic of China*

Youcai Qin − *State Key Laboratory for Biology of Plant Diseases and Insect Pests/Key Laboratory of Control of Biological Hazard Factors (Plant Origin) for Agri-product Quality and Safety, Ministry of Agriculture, Institute of Plant Protection, Chinese Academy of Agricultural Sciences, Beijing 100081, People's Republic of China*

Xiufen Yang − *State Key Laboratory for Biology of Plant Diseases and Insect Pests/Key Laboratory of Control of Biological Hazard Factors (Plant Origin) for Agri-product Quality and Safety, Ministry of Agriculture, Institute of Plant Protection, Chinese Academy of Agricultural Sciences, Beijing 100081, People's Republic of China*

Jie Ren − *State Key Laboratory for Biology of Plant Diseases and Insect Pests/Key Laboratory of Control of Biological Hazard Factors (Plant Origin) for Agri-product Quality and Safety, Ministry of Agriculture, Institute of Plant Protection, Chinese Academy of Agricultural Sciences, Beijing 100081, People's Republic of China*

Complete contact information is available at: https://pubs.acs.org/10.1021/acsomega.0c02357

Author Contributions

Y.D., J.R., and G.L. designed the study. Y.D., X.L., J.D., Y.Q., and X.Y. performed the experiments. Y.D., J.R., and G.L. wrote the manuscript. All authors read and approved the final manuscript.

Notes

The authors declare no competing financial interest.

■ ACKNOWLEDGMENTS

G.L. thanks the financial support from the National Natural Science Foundation of China (Grant No. 31972327), Agricultural Science and Technology Innovation Program of CAAS (CAAS-ZDRW202011), and the Elite Youth Program of the Chinese Academy of Agriculture Sciences.

■ ABBREVIATIONS USED

Xcn1, xenocoumacin 1; Xcn2, xenocoumacin 2; Xcn5, xenocoumacin 5; Xcn6, xenocoumacin 6; ISPR, in situ product removal; IJ, infective juvenile; NRPs, nonribosomal peptide synthetases; MTT, 3-(4,5-dimethylthiazol-2-yl)−2,5-diphenyltetrazolium bromide; DNS, 3, 5-dinitrosalicylic acid; RT-qPCR, real-time quantitative PCR; QC, quality control; RT, retention time; PCA, principle component analysis; OPLS-DA, orthogonal partial least-squares discriminant analysis; VIP, variable influence on projection; CID, compound identification number; UPLC−MS, ultrahigh-performance liquid chromatography−mass spectrometry

■ REFERENCES

(1) Shi, Y. M.; Bode, H. B. Chemical language and warfare of bacterial natural products in bacteria-nematode-insect interactions. *Nat. Prod. Rep.* **2018**, *35*, 309−335.

(2) Herbert, E. E.; Goodrich-Blair, H. Friend and foe: the two faces of *Xenorhabdus nematophila*. *Nat. Rev. Microbiol.* **2007**, *5*, 634−646.

(3) Forst, S.; Nealson, K. Molecular biology of the symbiotic-pathogenic bacteria *Xenorhabdus* spp. and *Photorhabdus* spp. *Microbiol. Rev.* **1996**, *60*, 21−43.

(4) Goodrich-Blair, H.; Clarke, D. J. Mutualism and pathogenesis in *Xenorhabdus* and *Photorhabdus*: two roads to the same destination. *Mol. Microbiol.* **2007**, *64*, 260−268.

(5) Goodrich-Blair, H. They've got a ticket to ride: *Xenorhabdus nematophila-Steinernema carpocapsae* symbiosis. *Curr. Opin. Microbiol.* **2007**, *10*, 225−230.

(6) Cao, M.; Patel, T.; Rickman, T.; Goodrich-Blair, H.; Hussa, E. A. High Levels of the *Xenorhabdus nematophila* Transcription Factor Lrp Promote Mutualism with the *Steinernema carpocapsae* Nematode Host. *Appl. Environ. Microbiol.* **2017**, *83*, No. e00276-17.

(7) Hillman, K.; Goodrich-Blair, H. Are you my symbiont? Microbial polymorphic toxins and antimicrobial compounds as honest signals of beneficial symbiotic defensive traits. *Curr. Opin. Microbiol.* **2016**, *31*, 184−190.

(8) Shi, H.; Zeng, H.; Yang, X.; Zhao, J.; Chen, M.; Qiu, D. An insecticidal protein from *Xenorhabdus ehlersii* triggers prophenoloxidase activation and hemocyte decrease in *Galleria mellonella*. *Curr. Microbiol.* **2012**, *64*, 604−610.

(9) Liu, H.; Zeng, H.; Yao, Q.; Yuan, J.; Zhang, Y.; Qiu, D.; Yang, X.; Yang, H.; Liu, Z. *Steinernema glaseri* surface enolase: molecular cloning, biological characterization, and role in host immune suppression. *Mol. Biochem. Parasitol.* **2012**, *185*, 89−98.

(10) Pan, Y. H.; Jian, H.; Zhang, J.; Liu, Z.; Huang, D. F. An intracellular toxic protein (Xin) isolated from *Xenorhabdus nematophilus* strain BJ. *Nat. Sci.* **2002**, *04*, 72−74.

(11) Snyder, H.; Stock, S. P.; Kim, S. K.; Flores-Lara, Y.; Forst, S. New insights into the colonization and release processes of *Xenorhabdus nematophila* and the morphology and ultrastructure of the bacterial receptacle of its nematode host, *Steinernema carpocapsae*. *Appl. Environ. Microbiol.* **2007**, *73*, 5338−5346.

(12) Richards, G. R.; Goodrich-Blair, H. Examination of *Xenorhabdus nematophila* lipases in pathogenic and mutualistic host interactions reveals a role for *xlpA* in nematode progeny production. *Appl. Environ. Microbiol.* **2010**, *76*, 221−229.

(13) Singh, S.; Orr, D.; Divinagracia, E.; McGraw, J.; Dorff, K.; Forst, S. Role of secondary metabolites in establishment of the mutualistic partnership between *Xenorhabdus nematophila* and the entomopathogenic nematode *Steinernema carpocapsae*. *Appl. Environ. Microbiol.* **2015**, *81*, 754−764.

(14) Tobias, N. J.; Heinrich, A. K.; Eresmann, H.; Wright, P. R.; Neubacher, N.; Backofen, R.; Bode, H. B. *Photorhabdus*-nematode symbiosis is dependent on *hfq*-mediated regulation of secondary metabolites. *Environ. Microbiol.* **2017**, *19*, 119−129.

(15) Muangpat, P.; Yooyangket, T.; Fukruksa, C.; Suwannaroj, M.; Yimthin, T.; Sitthisak, S.; Chantratita, N.; Vitta, A.; Tobias, N. J.; Bode, H. B.; Thanwisai, A. Screening of the Antimicrobial Activity against Drug Resistant Bacteria of *Photorhabdus* and *Xenorhabdus* Associated with Entomopathogenic Nematodes from Mae Wong National Park, Thailand. *Front. Microbiol.* **2017**, *8*, No. 1142.

(16) Cai, X.; Challinor, V. L.; Zhao, L.; Reimer, D.; Adihou, H.; Grun, P.; Kaiser, M.; Bode, H. B. Biosynthesis of the Antibiotic Nematophin and Its Elongated Derivatives in Entomopathogenic Bacteria. *Org. Lett.* **2017**, *19*, 806−809.

(17) Bozhüyük, K. A. J.; Zhou, Q.; Engel, Y.; Heinrich, A.; Perez, A.; Bode, H. B. Natural Products from *Photorhabdus* and Other Entomopathogenic Bacteria. In *The Molecular Biology of Photorhabdus Bacteria*; Current Topics in Microbiology and Immunology; Springer: Cham, 2017; Vol. *402*, pp 55−79.

(18) Nollmann, F. I.; Heinrich, A. K.; Brachmann, A. O.; Morisseau, C.; Mukherjee, K.; Casanova-Torres, A. M.; Strobl, F.; Kleinhans, D.; Kinski, S.; Schultz, K.; Beeton, M. L.; Kaiser, M.; Chu, Y. Y.; Phan Ke, L.; Thanwisai, A.; Bozhuyuk, K. A.; Chantratita, N.; Gotz, F.; Waterfield, N. R.; Vilcinskas, A.; Stelzer, E. H.; Goodrich-Blair, H.; Hammock, B. D.; Bode, H. B. A *Photorhabdus* natural product inhibits

insect juvenile hormone epoxide hydrolase. *ChemBioChem* **2015**, *16*, 766−771.
(19) Bode, H. B. Entomopathogenic bacteria as a source of secondary metabolites. *Curr. Opin. Chem. Biol.* **2009**, *13*, 224−230.
(20) Li, J.; Chen, G.; Webster, J. M.; Czyzewska, E. Antimicrobial metabolites from a bacterial symbiont. *J. Nat. Prod.* **1995**, *58*, 1081−1086.
(21) Martens, E. C.; Heungens, K.; Goodrich-Blair, H. Early colonization events in the mutualistic association between *Steinernema carpocapsae* nematodes and *Xenorhabdus nematophila* bacteria. *J. Bacteriol.* **2003**, *185*, 3147−3154.
(22) Furgani, G.; Boszormenyi, E.; Fodor, A.; Mathe-Fodor, A.; Forst, S.; Hogan, J. S.; Katona, Z.; Klein, M. G.; Stackebrandt, E.; Szentirmai, A.; Sztaricskai, F.; Wolf, S. L. *Xenorhabdus* antibiotics: a comparative analysis and potential utility for controlling mastitis caused by bacteria. *J. Appl. Microbiol.* **2008**, *104*, 745−758.
(23) Tobias, N. J.; Shi, Y. M.; Bode, H. B. Refining the Natural Product Repertoire in Entomopathogenic Bacteria. *Trends Microbiol.* **2018**, *26*, 833−840.
(24) Tobias, N. J.; Wolff, H.; Djahanschiri, B.; Grundmann, F.; Kronenwerth, M.; Shi, Y. M.; Simonyi, S.; Grun, P.; Shapiro-Ilan, D.; Pidot, S. J.; Stinear, T. P.; Ebersberger, I.; Bode, H. B. Natural product diversity associated with the nematode symbionts *Photorhabdus* and *Xenorhabdus*. *Nat. Microbiol.* **2017**, *2*, 1676−1685.
(25) Cai, X.; Nowak, S.; Wesche, F.; Bischoff, I.; Kaiser, M.; Furst, R.; Bode, H. B. Entomopathogenic bacteria use multiple mechanisms for bioactive peptide library design. *Nat. Chem.* **2017**, *9*, 379−386.
(26) Zhang, S.; Liu, Q.; Han, Y.; Han, J.; Yan, Z.; Wang, Y.; Zhang, X. Nematophin, an Antimicrobial Dipeptide Compound From *Xenorhabdus nematophila* YL001 as a Potent Biopesticide for *Rhizoctonia solani* Control. *Front. Microbiol.* **2019**, *10*, No. 1765.
(27) Lang, G.; Kalvelage, T.; Peters, A.; Wiese, J.; Imhoff, J. F. Linear and cyclic peptides from the entomopathogenic bacterium *Xenorhabdus nematophilus*. *J. Nat. Prod.* **2008**, *71*, 1074−1077.
(28) Li, J.; Chen, G.; Webster, J. M. Nematophin, a novel antimicrobial substance produced by *Xenorhabdus nematophilus* (Enterobactereaceae). *Can. J. Microbiol.* **1997**, *43*, 770−773.
(29) Gualtieri, M.; Aumelas, A.; Thaler, J. O. Identification of a new antimicrobial lysine-rich cyclolipopeptide family from *Xenorhabdus nematophila*. *J. Antibiot.* **2009**, *62*, 295−302.
(30) McInerney, B. V.; Taylor, W. C.; Lacey, M. J.; Akhurst, R. J.; Gregson, R. P. Biologically active metabolites from *Xenorhabdus* spp., Part 2. Benzopyran-1-one derivatives with gastroprotective activity. *J. Nat. Prod.* **1991**, *54*, 785−795.
(31) Maxwell, P. W.; Chen, G.; Webster, J. M.; Dunphy, G. B. Stability and Activities of Antibiotics Produced during Infection of the Insect *Galleria mellonella* by Two Isolates of *Xenorhabdus nematophilus*. *Appl. Environ. Microbiol.* **1994**, *60*, 715−721.
(32) Park, D.; Ciezki, K.; van der Hoeven, R.; Singh, S.; Reimer, D.; Bode, H. B.; Forst, S. Genetic analysis of xenocoumacin antibiotic production in the mutualistic bacterium *Xenorhabdus nematophila*. *Mol. Microbiol.* **2009**, *73*, 938−949.
(33) Reimer, D.; Pos, K. M.; Thines, M.; Grun, P.; Bode, H. B. A natural prodrug activation mechanism in nonribosomal peptide synthesis. *Nat. Chem. Biol.* **2011**, *7*, 888−890.
(34) Guo, S.; Zhang, S.; Fang, X.; Liu, Q.; Gao, J.; Bilal, M.; Wang, Y.; Zhang, X. Regulation of antimicrobial activity and xenocoumacins biosynthesis by pH in *Xenorhabdus nematophila*. *Microb. Cell Fact.* **2017**, *16*, No. 203.
(35) Reimer, D.; Luxenburger, E.; Brachmann, A. O.; Bode, H. B. A new type of pyrrolidine biosynthesis is involved in the late steps of xenocoumacin production in *Xenorhabdus nematophila*. *ChemBioChem* **2009**, *10*, 1997−2001.
(36) Yang, X.; Qiu, D.; Yang, H.; Liu, Z.; Zeng, H.; Yuan, J. Antifungal activity of xenocoumacin 1 from *Xenorhabdus nematophilus* var. pekingensis against *Phytophthora infestans*. *World J. Microbiol. Biotechnol.* **2011**, *27*, 523−528.
(37) Austin Bourke, P. M. Emergence of Potato Blight, 1843-46. *Nature* **1964**, *203*, 805−808.
(38) Huang, W.; Yang, X.; Yang, H.; Liu, Z.; Yuan, J. Identification and activity of Antibacterial substance from *Xenorhabdus nematophila* var. Pekingense. *Tianran Chanwu Yanjiu Yu Kaifa* **2006**, *18*, 25−28.
(39) Van Hecke, W.; Kaur, G.; De Wever, H. Advances in in-situ product recovery (ISPR) in whole cell biotechnology during the last decade. *Biotechnol. Adv.* **2014**, *32*, 1245−1255.
(40) Freeman, A.; Woodley, J. M.; Lilly, M. D. In situ product removal as a tool for bioprocessing. *Nat. Biotechnol.* **1993**, *11*, 1007−1012.
(41) Stark, D.; von Stockar, U. In situ product removal (ISPR) in whole cell biotechnology during the last twenty years. In *Process Integration in Biochemical Engineering*; Advances in Biochemical Engineering/Biotechnology; Springer: Berlin, Heidelberg, 2003; Vol. *80*, pp 149−175.
(42) Li, S. Y.; Chiang, C. J.; Tseng, I. T.; He, C. R.; Chao, Y. P. Bioreactors and in situ product recovery techniques for acetone-butanol-ethanol fermentation. *FEMS Microbiol. Lett.* **2016**, *363*, No. fnw107.
(43) Dafoe, J. T.; Daugulis, A. J. In situ product removal in fermentation systems: improved process performance and rational extractant selection. *Biotechnol. Lett.* **2014**, *36*, 443−460.
(44) Park, D.; Forst, S. Co-regulation of motility, exoenzyme and antibiotic production by the EnvZ-OmpR-FlhDC-FliA pathway in *Xenorhabdus nematophila*. *Mol. Microbiol.* **2006**, *61*, 1397−1412.
(45) Jiménez, J. J.; Borrero, J.; Diep, D. B.; Gutiez, L.; Nes, I. F.; Herranz, C.; Cintas, L. M.; Hernandez, P. E. Cloning, production, and functional expression of the bacteriocin sakacin A (SakA) and two SakA-derived chimeras in lactic acid bacteria (LAB) and the yeasts *Pichia pastoris* and *Kluyveromyces lactis*. *J. Ind. Microbiol. Biotechnol.* **2013**, *40*, 977−993.
(46) Trinetta, V.; Morleo, A.; Sessa, F.; Iametti, S.; Bonomi, F.; Ferranti, P. Purified sakacin A shows a dual mechanism of action against *Listeria* spp: proton motive force dissipation and cell wall breakdown. *FEMS Microbiol. Lett.* **2012**, *334*, 143−149.
(47) Hsiao, P. C.; Liaw, C. C.; Hwang, S. Y.; Cheng, H. L.; Zhang, L. J.; Shen, C. C.; Hsu, F. L.; Kuo, Y. H. Antiproliferative and hypoglycemic cucurbitane-type glycosides from the fruits of *Momordica charantia*. *J. Agric. Food Chem.* **2013**, *61*, 2979−2986.
(48) Fanali, S.; Aturki, Z.; Kasicka, V.; Raggi, M. A.; D'Orazio, G. Enantiomeric separation of mirtazapine and its metabolites by nano-liquid chromatography with UV-absorption and mass spectrometric detection. *J. Sep. Sci.* **2005**, *28*, 1719−1728.
(49) Bachi, A.; Brambilla, R.; Fanelli, R.; Bianchi, R.; Zuccato, E.; Chiabrando, C. Reduction of urinary 8-epi-prostaglandin F_{2a} during cyclo-oxygenase inhibition in rats but not in man. *Br. J. Pharmacol.* **1997**, *121*, 1770−1774.
(50) Huang, W.; Zhu, C.; Yang, X.; Yang, H.; Xu, H.; Xie, Y.; Jian, H. Isolation and structural identification of main component CB6-1 produced by *Xenorhabdus nematophilus* var pekingensis. *Zhongguo Kangshengsu Zazhi* **2005**, *9*, 513−515.
(51) Yu, J.; Yang, H.; Li, K.; Ren, H.; Lei, J.; Huang, C. Development of Epigallocatechin-3-gallate-Encapsulated Nanohydroxyapatite/Mesoporous Silica for Therapeutic Management of Dentin Surface. *ACS. Appl. Mater. Interfaces* **2017**, *9*, 25796−25807.
(52) Phwan, C. K.; Chew, K. W.; Sebayang, A. H.; Ong, H. C.; Ling, T. C.; Malek, M. A.; Ho, Y. C.; Show, P. L. Effects of acids pretreatment on the microbial fermentation process for bioethanol production from microalgae. *Biotechnol. Biofuels* **2019**, *12*, No. 191.
(53) Shang, R.; Pu, X.; Xu, X.; Xin, Z.; Zhang, C.; Guo, W.; Liu, Y.; Liang, J. Synthesis and biological activities of novel pleuromutilin derivatives with a substituted thiadiazole moiety as potent drug-resistant bacteria inhibitors. *J. Med. Chem.* **2014**, *57*, 5664−5678.
(54) Jiao, S.; Nie, M.; Song, H.; Xu, D.; You, F. Physiological responses to cold and starvation stresses in the liver of yellow drum (*Nibea albiflora*) revealed by LC-MS metabolomics. *Sci. Total Environ.* **2020**, *715*, No. 136940.
(55) Boccard, J.; Rutledge, D. N. A consensus orthogonal partial least squares discriminant analysis (OPLS-DA) strategy for multiblock Omics data fusion. *Anal. Chim. Acta* **2013**, *769*, 30−39.

https://dx.doi.org/10.1021/acsomega.0c02357
ACS Omega 2020, 5, 20391−20398